

# Two Views Are Better than One: Monocular 3D Pose Estimation with Multiview Consistency

Christian Keilstrup Ingwersen<sup>1,2</sup>

Anders BJORHOLM DAHL<sup>1</sup>

Janus NØRTOFT JENSEN<sup>1</sup>

Morten RIEGER HANNEMOSE<sup>1</sup>

<sup>1</sup> Visual Computing, Technical University of Denmark

<sup>2</sup> TrackMan A/S, Denmark

cin@trackman.com, {abda, jnje, mohan}@dtu.dk

## Abstract

Deducing a 3D human pose from a single 2D image or 2D keypoints is inherently challenging, given the fundamental ambiguity wherein multiple 3D poses can correspond to the same 2D representation. The acquisition of 3D data, while invaluable for resolving pose ambiguity, is expensive and requires an intricate setup, often restricting its applicability to controlled lab environments. We improve performance of monocular human pose estimation models using multiview data for fine-tuning. We propose a novel loss function, multiview consistency, to enable adding additional training data with only 2D supervision. This loss enforces that the inferred 3D pose from one view aligns with the inferred 3D pose from another view under similarity transformations. Our consistency loss substantially improves performance for fine-tuning with no available 3D data. Our experiments demonstrate that two views offset by 90 degrees are enough to obtain good performance, with only marginal improvements by adding more views. Thus, we enable the acquisition of domain-specific data by capturing activities with off-the-shelf cameras, eliminating the need for elaborate calibration procedures. This research introduces new possibilities for domain adaptation in 3D pose estimation, providing a practical and cost-effective solution to customize models for specific applications. The used dataset, featuring additional views, will be made publicly available.

## 1. Introduction

Monocular 3D pose estimation is a pivotal task within computer vision, with applications across various domains such as augmented reality, human-computer interaction, robotics, and sports analytics. However, inferring a 3D human pose from a single 2D image or from 2D keypoints is fundamentally an ambiguous problem, with multiple 3D

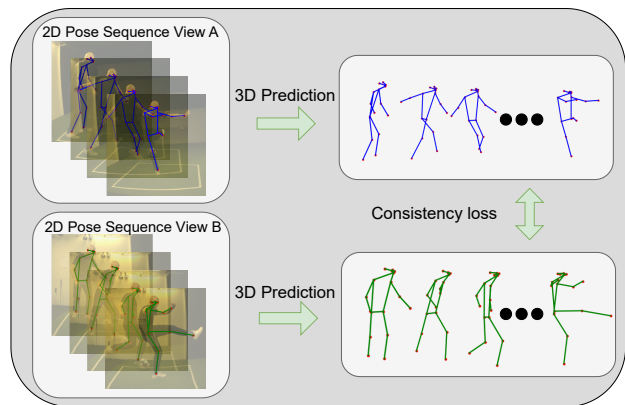


Figure 1. We utilize multiple sequences captured from different views to improve monocular performance by incorporating a consistency loss during training. The consistency loss penalizes variations between two predicted pose sequences of the same activity. We only use multiple views during training.

poses having the exact same 2D representation.

With this inherent ambiguity, models inferring 3D pose need an underlying representation of how the body can move and, ideally, which movements it can expect to see. To introduce such a prior in the model, it has become popular to rely on large foundation models [36] which have learned good priors of how the body generally moves. Creating well-performing models on datasets that contain less frequently seen movements often requires fine-tuning the foundation models for the specific domain and set of movements [36].

Methods for adapting 3D human pose models to different domains and movements have traditionally relied on the availability of new 3D data [14, 34, 35]. However, it is costly and may not be feasible to set up systems for capturing 3D data. To address these challenges, alternative methods have been explored. These methods have demonstrated

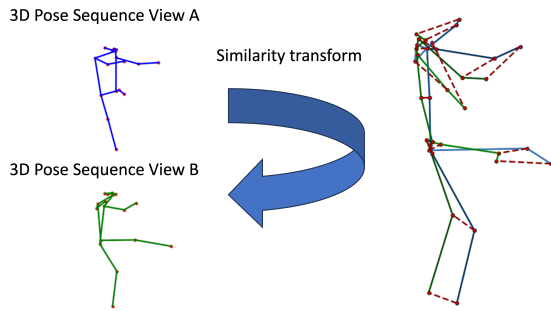


Figure 2. For every predicted 3D pose sequence obtained from View A and View B, we compute a similarity transform with Procrustes Analysis. This transformation aligns the predicted poses in sequence A with sequence B. The consistency loss is the average distance between the two pose sequences post-alignment, illustrated as dashed red lines. Using Procrustes analysis for this transformation enables us to use cameras with unknown intrinsics and extrinsics.

that 3D pose models can be fine-tuned using 2D data, as suggested by previous work [1]. This fine-tuning process involves ensuring that the inferred 3D joint positions align with 2D keypoints in an image, which can be obtained accurately using readily available methods [12, 32]. However, since we, in the end, want a good 3D representation, it is not ideal to rely only on 2D supervision, as it has been shown that models tend to forget the depth representation [7].

To advance fine-tuning with purely 2D supervision, we introduce a new loss function that enforces multiview consistency, requiring the inferred 3D pose from one view to be close to the inferred 3D pose from another view under a similarity transform. Figure 1 sketches the concept of the consistency loss detailed in Figure 2.

While we focus on increasing the performance of monocular models and not models utilizing multiple views, we recognize that many datasets used for training monocular models have multiple views of the scene available [8, 13, 22, 24]. Multiple views are typically not utilized while training the models. We demonstrate the feasibility of our loss and the improvements that can be obtained by using multiple views during training while only using a single view at inference time. Additionally, we investigate how many views are necessary to obtain improvements in 3D predictions. In this study, we use the SportsPose dataset [8], containing multiple dynamic movements. The authors provided us with full access to all seven views of this dataset, and we will release these together with this paper. The SportsPose dataset features complex and challenging sports scenarios, making it an ideal test bed for our domain-adaptive approach. The new views are available on our web-

site<sup>1</sup>.

While we demonstrate our loss on the SportsPose dataset [8], which contains ground truth 3D data as well as a full multi-camera calibration, we only utilize the 2D joint information for training and use the 3D data purely for evaluation. Because of the similarity transformation, our view-consistency loss eliminates the need for calibrated cameras, offering a significant advantage in scenarios where camera calibration is impractical or unobtainable. Moreover, it effectively resolves the inherent ambiguity associated with fine-tuning on 2D label data. When using 2D label data for training, the model can be confounded by multiple different 3D points that project to the same 2D coordinates. Our multiview consistency loss provides a robust solution to this challenge, substantially enhancing the accuracy and reliability of monocular 3D pose estimation.

Our contributions extend beyond introducing the view-consistency loss for domain-adaptive 3D pose estimation. We also present the first set of baseline results on the SportsPose dataset, demonstrating the effectiveness of our approach. We illustrate how our method enhances 3D pose estimation accuracy in dynamic and complex environments by showcasing a model fine-tuned on the SportsPose dataset. This research opens up new possibilities for domain adaptation in 3D pose estimation, providing a practical and cost-effective solution to customize models for specific applications.

## 2. Related work

### 2.1. Monocular 3D human pose models

In the domain of monocular 3D human pose estimation, two primary approaches exist. One focuses solely on determining the 3D joint locations of the body [25, 28, 34], while the other includes estimating the body shape [1, 14, 17, 18, 33]. The latter category often employs parametric body models such as SMPL [21], which describes the body through shape parameters and pose parameters. Notably, even when applied to datasets without explicit shape parameters, our proposed loss remains applicable to methods estimating SMPL coefficients, as the consistency requirement across views applies to both 3D joint positions and shape parameters.

Irrespective of whether the goal is to estimate pose alone or to include shape parameters, monocular 3D human pose estimation commonly adopts either a one-stage or a two-stage approach. In one-stage approaches, the estimation is directly derived from an image or video input, while two-stage approaches involve lifting estimated 2D poses to 3D space. State-of-the-art monocular models that employ the two-stage approach, lifting 2D poses to 3D, achieve remarkable mean per joint precision errors (MPJPE [7]). They reach as low as 17mm [36] when lifting ground truth 2D

<sup>1</sup>Will be available soon.

poses on the Human3.6M dataset [9], and 37mm when lifting estimated 2D poses [36].

Models that adopt the alternative approach, by inferring the 3D pose by estimating the parametric SMPL model directly from image input, have achieved remarkable MPJPE scores of 60mm [29] on the in-the-wild 3DPW dataset [31].

## 2.2. Multiview 3D human pose models and datasets

Multiple synchronized and calibrated cameras have been extensively used in human pose estimation work [2, 11, 26]. Utilizing calibrated camera setups in such approaches has yielded impressive results, even generating state-of-the-art 3D human pose datasets [8, 13, 22, 24]. These datasets, in turn, play a pivotal role in training and advancing monocular models. However, the practical implementation of multicamera setups involves intricate calibration and synchronization processes, which often confines data to be collected in controlled laboratory environments.

Approaches that require limited or no 3D supervision have also been explored [5, 10, 16, 20, 23]. Liu et al. [20] require a fully calibrated camera setup to predict pose. Others do not require known camera extrinsics but, instead, estimate relative camera poses by decomposing the essential matrix estimated from 2D poses predicted in multiple views. Then the 3D pose is triangulated using the estimated relative poses, which are then used as training data [5, 16]. Mitra et al. [23] add additional training data from multiview images and use metric learning to enforce that images of the same pose have similar embeddings. The approach of Iqbal et al. [10] is most similar to ours, but they require known camera intrinsics. They infer 3D poses with a monocular model from multiple views and align them rigidly. During training, they penalize the model for differences in the predicted poses. However, the latter two approaches apply only single images for multiview consistency and not sequences, greatly limiting their potential.

## 3. Multiview consistency loss

Instead of relying on a known intrinsic calibration, our consistency loss can be deployed without any prior information about the cameras. To avoid using a calibration, the consistency loss applies a similarity transformation and penalizes differences in the poses of two sequences of the same activity, see Figure 2. Avoiding camera calibration simplifies the training pipeline and gives an efficient alternative for handling data from multiple views.

Specifically, the loss is based on the difference between poses computed from two or more views after alignment with a similarity transformation,  $\tau$ . We compute the mean

over every pair of two cameras, which results in the loss

$$\mathcal{L}_{\text{con}} = \sum_{s=1}^S \frac{1}{|V_s|} \sum_{(a,b) \in V_s} \mathcal{L}_c(\hat{J}_a, \hat{J}_b). \quad (1)$$

Here  $S$  is the total number of sequences and  $V_s$  is the set of possible pairs of views of the sequence  $s$ . Therefore, with  $N$  different cameras available in a sequence,  $|V_s| = \binom{N}{2}$ . The consistency loss  $\mathcal{L}_c$  is calculated between  $\hat{J}_a$  and  $\hat{J}_b$ , which are the predicted 3D body joints for all frames of the sequence from view  $a$  and view  $b$ , respectively. The term  $\mathcal{L}_c$  is computed as follows

$$\mathcal{L}_c(\hat{J}_a, \hat{J}_b) = \frac{1}{n} \sum_{i=1}^n \left\| \tau(\hat{J}_{a,i}; \hat{\theta}_{ab}) - \hat{J}_{b,i} \right\|_2, \quad (2)$$

where  $\hat{J}_{a,i}$  is element  $i$ , from the sequence of predicted 3D poses from view  $a$ , which has length  $n$ . Similarly  $\hat{J}_{b,i}$  is element  $i$  from the sequence of predicted 3D poses from view  $b$ .  $\tau$  is a similarity transform with parameters  $\hat{\theta}_{ab}$  that are estimated such that  $\tau$  transforms  $\hat{J}_{a,i}$  to be as close as possible to  $\hat{J}_{b,i}$  by scaling, rotating and translating the 3D joints from  $\hat{J}_{a,i}$ .

To compute the scaling, rotation, and translation used to transform  $\hat{J}_{a,i}$ , we estimate the optimal parameters,  $\hat{\theta}_{ab}$ , as in Equation (3). Here it should be noted that contrary to how similarity transformations traditionally are computed in 3D human pose estimation to compute the Procrustes aligned MPJPE, we only compute one transformation,  $\hat{\theta}_{ab}$ , for the entire sequence and not one per pose as in the PA-MPJPE metric [7].

$$\hat{\theta}_{ab} = \arg \min_{\theta} \sum_{i=1}^n \left\| \tau(\hat{J}_{a,i}; \theta) - \hat{J}_{b,i} \right\|_2^2. \quad (3)$$

The optimal solution to Equation (3) is found using Procrustes analysis [6], such that we obtain the optimal scaling, rotation, and translation to transform  $\hat{J}_{a,i}$  as follows

$$\tau(\hat{J}_{a,i}; \hat{\theta}_{ab}) = s \hat{J}_{a,i} R + t. \quad (4)$$

By transforming  $\hat{J}_a$ , the idea is to directly estimate the similarity transformation that transforms from the camera coordinate system of camera  $a$  to the coordinate system of camera  $b$  instead of relying on knowing the camera extrinsics in order to perform the transformation.

## 4. Experiments

### 4.1. Test protocol

To evaluate our proposed consistency loss, as defined in Equation (1), we conduct experiments using the SportsPose dataset [8]. Since the original paper does not provide a

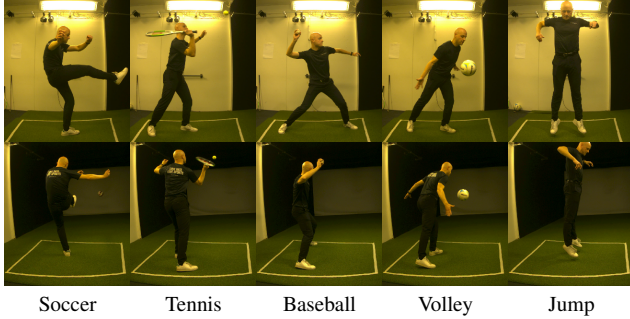


Figure 3. The five activities from SportsPose [8]. The top row displays the publicly available view “right”, while the bottom row features a view rotated 90-degrees relative to “right”, which we refer to as “View 1”.

specified test protocol, we employ a test protocol inspired by Human3.6M [9], wherein subjects are distributed across sets to ensure that no subject appears in the same set.

For validation purposes, we use subjects S04, S07, S09, S14, and S22. Subsequently, for testing, we employ subjects S06, S12, and S19. To focus on monocular performance, we opt to use only the current available view, “right”, during both testing and validation of the model. This decision streamlines the evaluation process, as we are interested in assessing the proficiency of the model when exposed to a single front-facing view. Examples of this view are in the first row of Figure 3.

## 4.2. Implementation

While our view-consistency loss is versatile and applicable to any monocular 3D human pose method, we choose to adapt the MotionBERT model by Zhu et al. [36] and fine-tuning it to the SportsPose [8] dataset.

To use SportsPose [8] with MotionBERT [36] we need to preprocess the data first. We convert the definition of body keypoints from COCO [19] keypoints used in SportsPose to the Human3.6M [9] body keypoint format. The keypoints are further transformed from meters to millimeters and by using the extrinsic camera parameters transformed from the world coordinate system to each of the cameras. Then, following the approach in [3], the camera coordinates are transformed to pixel coordinates and scaled to be within the range  $[-1; 1]$ .

For the fine-tuning of MotionBERT [36], we employ the weights provided for the DSTformer with a depth of five and eight heads. The sequence length is 243, and both the feature and embedding sizes are 512. Adhering to the training protocol suggested by Zhu et al. [36], we fine-tune the models for 30 epochs, using a learning rate of 0.0002 and utilizing the Adam optimizer [15].

## 4.3. Fine-tuning with 3D data

When the ground truth 3D data is available, we implement the proposed fine-tuning configuration from MotionBERT. This involves using a positional loss,  $\mathcal{L}_{\text{pos}}$  directly on the 3D poses, coupled with losses on joint velocities,  $\mathcal{L}_{\text{vel}}$ , and scale only loss,  $\mathcal{L}_{\text{scale}}$ , as suggested by Rhodin et al. [27]. This combination results in the combined loss for 3D data,

$$\mathcal{L}_{3D} = \lambda_{\text{pos}}\mathcal{L}_{\text{pos}} + \lambda_{\text{vel}}\mathcal{L}_{\text{vel}} + \lambda_{\text{scale}}\mathcal{L}_{\text{scale}}, \quad (5)$$

where  $\lambda_{\text{pos}}$ ,  $\lambda_{\text{vel}}$ , and  $\lambda_{\text{scale}}$  are weights for the respective losses. Our proposed consistency loss is added as a regularization term,  $\lambda_{\text{con}}\mathcal{L}_{\text{con}}$ , to the total loss, resulting in Equation (6),

$$\mathcal{L}_{3D_{\text{con}}} = \lambda_{\text{pos}}\mathcal{L}_{\text{pos}} + \lambda_{\text{vel}}\mathcal{L}_{\text{vel}} + \lambda_{\text{scale}}\mathcal{L}_{\text{scale}} + \lambda_{\text{con}}\mathcal{L}_{\text{con}}. \quad (6)$$

After an extensive parameter search, aligning with suggestions from Zhu et al. [36], we identify the optimal configuration for Equation (6) as  $\lambda_{\text{pos}} = 1$ ,  $\lambda_{\text{vel}} = 20$ ,  $\lambda_{\text{scale}} = 0.5$ , and  $\lambda_{\text{con}} = 0.2$ . These parameters are employed to obtain the results presented in Table 1, utilizing two camera views from SportsPose [8], one from the right side, as illustrated in the first row of Figure 3, and another 90 degrees to the view facing the back of the subject as in the second row of Figure 3. The second view behind the subject is based on the assumption that this view contains the most information when joints are occluding each other in the original “right” view from SportsPose [8].

The results in Table 1 showcase the impact of the consistency loss on model performance. When ground truth 3D data is available, the consistency loss yields marginal improvements, with 0.8mm decrease in MPJPE and 0.2mm in PA-MPJPE. However, this slight enhancement suggests that our regularization term can be seamlessly integrated, even when 3D data are accessible, without compromising performance.

In cases where 3D human pose data is accessible, the impact of the consistency loss on accuracy is relatively modest. However, it is crucial to emphasize that our consistency loss is intentionally crafted for scenarios lacking 3D data. This underscores its utility as a valuable regularization technique for monocular pose estimation, acknowledging that the efficacy of 3D data remains superior to achieve a well-performing model.

## 4.4. Fine-tuning without available 3D data

In situations where ground truth 3D joint data is unavailable, refining a model through fine-tuning is still possible. This fine-tuning involves reprojecting the predicted 3D

	Soccer kick		Tennis serve		Baseball pitch		Volley		Jumping		All	
	MPJPE	PA	MPJPE	PA	MPJPE	PA	MPJPE	PA	MPJPE	PA	MPJPE	PA
<b>Baseline</b>												
MotionBERT [36]	55.3	32.8	69.4	41.3	71.3	34.6	65.2	33.1	71.1	45.3	65.0	37.3
<b>Fine-tuning with 3D data (2 views)</b>												
$\mathcal{L}_{3D}$ (5)	15.4	11.3	16.2	12.0	15.9	11.4	15.5	10.5	16.6	<b>12.3</b>	15.6	11.5
$\mathcal{L}_{3D_{con}}$ (6), Ours	<b>14.4</b>	<b>11.2</b>	<b>15.8</b>	<b>11.8</b>	<b>14.3</b>	<b>10.6</b>	<b>13.4</b>	<b>9.9</b>	<b>16.3</b>	12.9	<b>14.8</b>	<b>11.3</b>
<b>Only 2D fine-tuning (2 views)</b>												
$\mathcal{L}_{2D}$ (7)	53.0	44.5	63.3	48.1	56.4	38.7	55.4	42.6	70.4	49.7	63.2	45.9
$\mathcal{L}_{2D_{con}}$ (8), Ours	<b>27.8</b>	<b>16.9</b>	<b>23.2</b>	<b>15.9</b>	<b>24.8</b>	<b>15.7</b>	<b>21.9</b>	<b>13.6</b>	<b>25.5</b>	<b>17.1</b>	<b>24.0</b>	<b>15.5</b>

Table 1. Results on SportsPose [8]. Baseline is MotionBERT [36], which is then fine-tuned with either 2D ( $\mathcal{L}_{2D}$ ) or 3D ( $\mathcal{L}_{3D}$ ) supervision with and without our proposed multiview consistency loss  $\mathcal{L}_{con}$ . All results in mm, lower is better. MPJPE is mean per joint precision error and PA is Procrustes aligned MPJPE. All results use ground truth 2D poses. **Bold** is best performance with only 2D data and **bold gray** is best performance overall. The two views can be seen in Figure 3. The consistency loss improves performance in both cases but substantially more when 3D supervision is not used.

points onto the image and assessing how well these reprojected keypoints align with the ground truth 2D keypoints. However, obtaining precise ground truth 2D poses, although less challenging than gathering 3D poses and not requiring specialized hardware, requires substantial effort and manual annotation.

In practice, the use of ground truth 2D poses is limited due to annotation challenges. Instead, models frequently leverage estimated 2D keypoints from detectors such as HRNet [30] or AlphaPose [4] for supervision. Notably, when employing estimated keypoints, the reprojection error is often weighted by the confidence scores provided by the 2D keypoint detectors. This strategy minimizes the impact of less reliable keypoints on the overall training process while maintaining the essential guidance for model refinement.

To validate the performance of our proposed consistency loss, we use the ground truth 2D poses from SportsPose [8] with the preprocessing described in Section 4, to fine-tune the MotionBERT [36] model. When fine-tuning the model without the consistency loss, we solely use the 2D reprojection loss,

$$\mathcal{L}_{2D} = \lambda_{2D_{reproj}} \mathcal{L}_{2D_{reproj}}. \quad (7)$$

Again we add the consistency loss as a regularization term resulting in the total loss in Equation (8). Through experimentation, we found that when two camera views are available, we achieve the best performance, with  $\lambda_{2D_{reproj}} = 1$  and  $\lambda_{con} = 0.3$ ,

$$\mathcal{L}_{2D_{con}} = \lambda_{2D_{reproj}} \mathcal{L}_{2D_{reproj}} + \lambda_{con} \mathcal{L}_{con}. \quad (8)$$

By fine-tuning the MotionBERT [36] model with the losses in Equation (7) and Equation (8), using two camera

views as described in Section 4.3, we achieve the results presented in Table 1.

The outcomes presented in Table 1 highlight the noteworthy impact of the consistency loss regularization term, particularly in scenarios where ground truth 3D information is absent. This regularization term leads to a substantial improvement in MPJPE, demonstrating a reduction of 39.2mm compared to relying solely on the reprojection loss. Visualizing 3D predictions from models with and without the consistency loss, Figure 4, we see the same substantial accuracy increase when using the consistency loss.

We believe this improvement is this big because the consistency loss has improved the network’s ability to resolve ambiguities during the process of lifting 2D to 3D from a single view. Additionally, it proves beneficial in situations where joints might be occluded in one of the views, enhancing the overall robustness of the model.

However, a closer examination of the Procrustes aligned joint error in Table 1 reveals an interesting observation. Fine-tuning the model solely on 2D body keypoints results in an increase in error. This phenomenon could be attributed to the inherent ambiguity associated with multiple different 3D poses that can reproject to the same 2D body pose. Consequently, the model may struggle to provide accurate depth estimates of joint locations, as highlighted in the work by Ingwersen et al. [7]. This underscores the importance of the consistency loss in mitigating such challenges and emphasizes its role in refining the model’s performance in the absence of ground truth 3D data.

#### 4.5. How many views do we need?

Examining the experiments carried out in Section 4.3 and Section 4.4, a logical inquiry arises regarding the scalability of the results when more than two views are incorporated

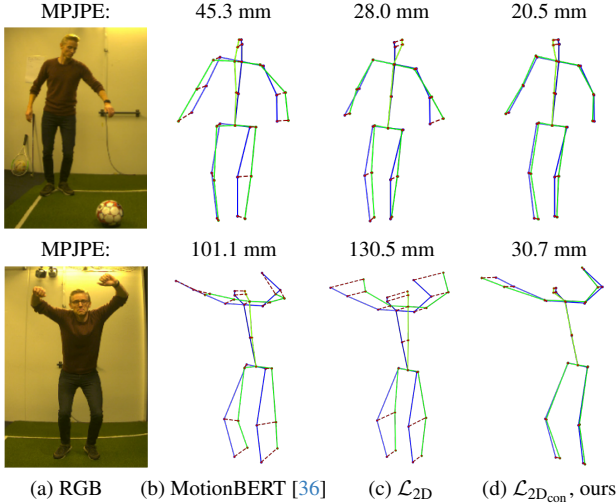


Figure 4. Visual comparison of predictions in green and the ground truth pose in blue. The magnitude of errors, measured in millimeters and indicated at the top, highlights the superiority of our consistency loss  $\mathcal{L}_{2D_{con}}$  in achieving more accurate results. The notable improvement is especially evident in the bottom row, where the method employing our consistency loss successfully captures the complex movement.

into the experiments. To investigate the correlation between the number of views and performance, we have calculated the results for scenarios where one to seven views are available, encompassing the total number of views in the Sports-Pose dataset [8].

#### 4.5.1 Without available 3D data

In the absence of ground-truth 3D data, the influence of including multiple views on accuracy is evident as shown in Section 4.4 and the results in Table 1. To compute the results that involve more than two views without access to 3D data, we utilize the loss function from Equation (8) with a consistent configuration, specifically setting  $\lambda_{2D_{reproj}} = 1$  and  $\lambda_{con} = 1$  for all experiments.

It is essential to note that this configuration is not fine-tuned for a specific number of views, which may result in variations compared to the results presented in Table 1. The outcome of this ablation study is detailed in Figure 5.

Examining the results for 2D supervision in Figure 5 reveals a substantial increase in accuracy as we progress from one to two views. However, the accuracy curve for both MPJPE and PA-MPJPE appears to plateau beyond two views, with marginal gains observed when incorporating more than two views.

This observed plateau could be attributed to diminishing returns in information gain beyond the second view. While

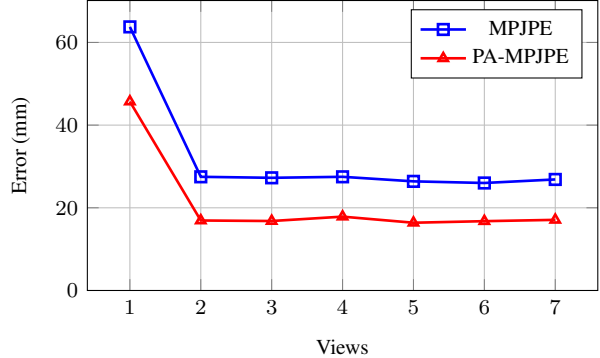


Figure 5. MPJPE and PA-MPJPE as function of views for experiments with  $\mathcal{L}_{2D_{con}}$  and a  $\lambda_{con}$  of 1. We see that with just two available views, the performance increases significantly. On the other hand, the performance does not further increase after two available views.

additional views contribute valuable perspectives, they may not necessarily introduce new information that significantly refines the precision of the predicted joints. Interestingly, this property of the loss underscores its utility, particularly in scenarios where capturing new data becomes significantly more manageable requiring only two views of the activity from an uncalibrated camera setup.

#### 4.5.2 With available 3D data

When 3D data is available, the incorporation of our consistency loss with two views, as illustrated in Section 4.3 and detailed in Table 1, does not result in a significant improvement in MPJPE or PA-MPJPE. However, a modest performance increase is observed, raising the question of whether this incremental gain will persist with an increasing number of views or reach a plateau, similar to the findings in Section 4.5.1.

In these experiments, we employ the loss function from Equation (6) with  $\lambda_{pos} = 1$ ,  $\lambda_{vel} = 20$ ,  $\lambda_{scale} = 0.5$ , and  $\lambda_{con} = 1$ . Notably, these values are not fine-tuned for any specific number of views and may thus differ from the results presented in Table 1. The outcomes of this experiment are illustrated in Figure 6.

Surprisingly, as depicted in Figure 6, we observe a decrease in performance when an additional view is added, along with the inclusion of our consistency loss. This contrasts with the findings in Table 1, where the consistency loss demonstrated performance improvement when included, while maintaining the number of views at two.

However, when we include all seven views, we do see a slight performance increase. Nonetheless, the variation in performance is generally small, and the overarching conclusion remains unchanged: when 3D data is available, there is no need to adapt the consistency loss.

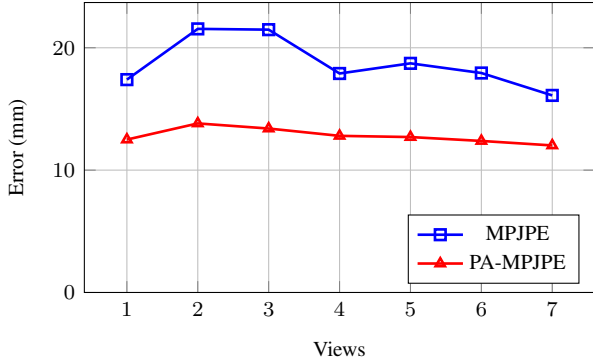


Figure 6. MPJPE and PA-MPJPE as function of views for experiments with  $\mathcal{L}_{3D_{con}}$  and a  $\lambda_{con}$  of 1. Although we do see a slight increase in performance when we include more views, the increase is far from as significant as when 3D data is not available.

#### 4.6. More views or more data?

Examining Figure 5 and Figure 6, one may question if the marginal accuracy improvements with 3D supervision, coupled with our consistency loss, and the substantial gains with 2D supervision are due to increased amount of training data or the impact of our consistency loss. To explore this we have conducted the same experiments but without including  $\mathcal{L}_{con}$  in the loss.

In the experiment analogous to 2D supervision illustrated in Figure 5, an examination of the results without the consistency loss in Figure 7 reveals that neither MPJPE nor PA-MPJPE exhibit improvement with the addition of more training data through an increased number of views. The consistent accuracy plateau observed contradicts the substantial accuracy increases depicted in Figure 5, suggesting that these improvements are primarily attributed to the introduction of our consistency loss.

However, examining the experiments adding data to the 3D supervision in Figure 8, we observe a trend similar to that depicted in Figure 6 with the error decreasing slightly when we add more data to the training. The error exhibits a slight decrease as more data is incorporated into the training process. This suggests that the marginal improvements in accuracy, observed when employing our consistency loss in conjunction with 3D supervision, can be attributed to the increased volume of data rather than solely to the presence of the consistency loss. This finding supports the overarching conclusion that 3D data is superior, and underscores that the true advantage of our consistency loss lies in enhancing accuracy in scenarios where obtaining 3D data is impractical.

#### 4.7. Which views to choose

In the experiments presented in Figures 5 and 6, the selection of views followed a deterministic process. Specifically,

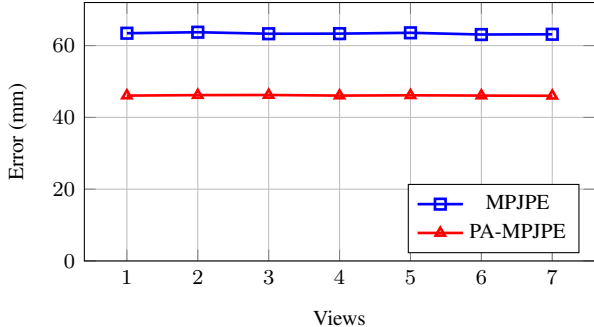


Figure 7. MPJPE and PA-MPJPE as functions of the number of views for experiments utilizing  $\mathcal{L}_{2D}$  exclusively. The aim is to discern whether the increase in accuracy observed in Figure 5 is influenced by the consistency loss or the augmented data availability. Notably, the nearly flat trends in both cases indicate that the accuracy boost associated with multiple views primarily stems from the incorporation of the consistency loss.

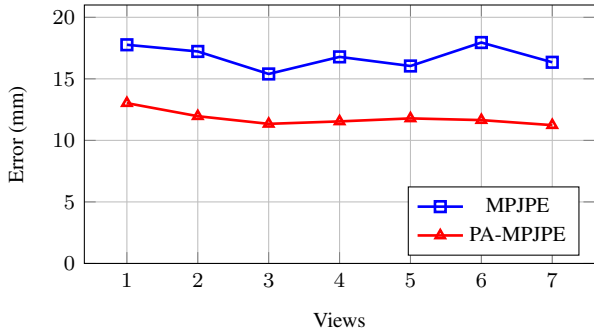


Figure 8. MPJPE and PA-MPJPE as functions of the number of views for experiments involving  $\mathcal{L}_{3D}$  without the consistency loss term. The purpose is to explore whether the marginal improvements in accuracy in Figure 6 are attributable to the consistency loss or the increased availability of data. Notably, we observe a decreasing trend in error as the number of views is augmented, even in the without the consistency loss.

the first view was consistently chosen as the “right” view from SportsPose [8], and the second view was the one positioned closest to a 90-degree angle relative to the initial view, facing the back of the subject. For scenarios involving three or more views, the remaining views were selected arbitrarily but maintained the same order across all experiments.

In Figure 9, the model is trained using the “right” view in combination with all other available views, where View 1 corresponds to the perspective positioned 90 degrees relative to the view facing the back of the subject.

Analyzing the errors depicted in Figure 9, it is evident that the choice of the view for multiview supervision significantly influences the outcomes of using our consistency loss. This intuitively aligns with expectations, as certain

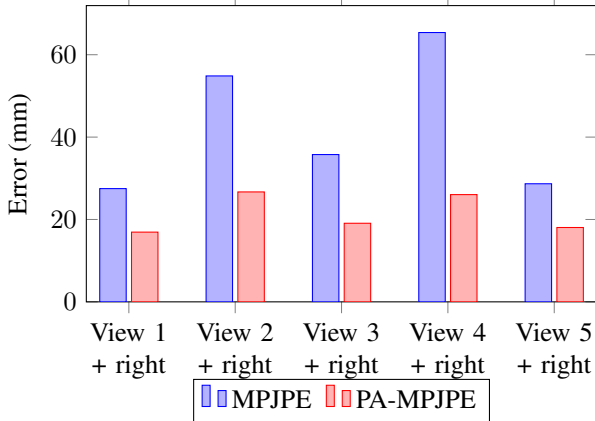


Figure 9. MPJPE and PA-MPJPE of different combinations of two views. The view “right” is included in all combinations. All experiments have been conducted with  $\mathcal{L}_{2D_{con}} = \lambda_{con} = 1$ . It is clear that the two-view combination matters with views 1 + right and view 5 + right achieving substantially lower errors.

views are more effective in resolving ambiguities and identifying occluded joints, while others may not contribute new information. The results indicate that an optimal configuration involves using views from two sides that are 90 degrees apart when only two cameras are available.

## 5. Consistency loss and parametric methods

As briefly mentioned in Section 2.1 the consistency loss can also be applicable when training models utilizing parametric body models such as SMPL [21].

Adapting the consistency loss for SMPL entails modifying Equation (2) to exclude the similarity transform. Additionally, we need two variants of the loss. One related to the shape parameters,  $\beta$

$$\mathcal{L}_c(\hat{\beta}_a, \hat{\beta}_b) = \frac{1}{n} \sum_{i=1}^n \left\| \hat{\beta}_{a,i} - \hat{\beta}_{b,i} \right\|_2, \quad (9)$$

and one related to the pose parameters,  $\theta$

$$\mathcal{L}_c(\hat{\theta}_a, \hat{\theta}_b) = \frac{1}{n} \sum_{i=1}^n \left\| \hat{\theta}_{a,i} - \hat{\theta}_{b,i} \right\|_2. \quad (10)$$

The modification of the losses, by excluding the similarity transform, is driven by the inherent invariance of the shape and pose parameters within the SMPL model when viewed from different perspectives. The constancy of these parameters across various views eliminates the necessity for any additional transformations.

Despite this invariance, the incorporation of multiple views of the same activity remains advantageous. Specifically, the human shape, denoted by  $\beta$ , exhibits constancy across different views, allowing us to penalize deviations

between predicted shapes from different views, represented as  $\hat{\beta}_a$  and  $\hat{\beta}_b$  for views A and B, respectively.

Similarly, as the pose parameters in SMPL describe relative joint rotations rather than joint positions, penalizing discrepancies between the predicted pose parameters  $\hat{\theta}_a$  and  $\hat{\theta}_b$  for views A and B becomes a meaningful constraint.

## 6. Discussion and conclusion

**Limitations.** While our results underscore a notable improvement in accuracy achieved through the implementation of our consistency loss, it is crucial to acknowledge certain unresolved limitations. As depicted in Figure 9, the efficacy of the consistency loss is contingent upon the selection of views for training, with the least favorable combination resulting in performance comparable to using a single camera view. However, a substantial increase in accuracy is evident in four out of five combinations.

Furthermore, it is essential to highlight that an excessive emphasis on the consistency loss, indicated by a large  $\lambda_{con}$  value, can lead to a degenerate solution. Specifically, an optimal solution to Equation (2) may manifest as predicting all zeroes, emphasizing the need for careful consideration when setting this parameter.

It is worth noting that the incorporation of the proposed consistency loss necessitates temporal synchronization of pose sequences from different views. This requirement imposes constraints on the camera system used for data capture. In future extensions of the consistency loss, exploring how temporal alignment can be integrated into the transformation between views would be a valuable addition.

**Conclusion.** We present a novel method to enhance monocular 3D human pose estimation performance. By incorporating our multiview consistency loss during training in scenarios where 3D data is unavailable, we achieve notable improvements in performance when compared to relying solely on a 2D reprojection loss or no fine-tuning.

A thorough analysis exploring various configurations involving the number of views and camera placement reveals that an effective enhancement is achieved with just two appropriately positioned views. We observe that positioning the cameras at a 90-degree angle yields consistently good performance compared to other combinations of views. This demonstrates that, through the use of our multiview consistency loss, it is feasible to capture new domain data for fine-tuning a model with a simple setup needing only two appropriately positioned and time-synchronized cameras.

With this paper, we also release six new views of sports activities to the SportsPose [8] dataset. Together with the new data we propose a new test protocol for the dataset and provide a simple baseline relying on MotionBERT [36] and our proposed consistency loss.



## References

- [1] Federica Bogo, Angjoo Kanazawa, Christoph Lassner, Peter Gehler, Javier Romero, and Michael J. Black. Keep it SMPL: Automatic estimation of 3D human pose and shape from a single image. In *Computer Vision – ECCV 2016*. Springer International Publishing, 2016. 2
- [2] Sungho Chun, Sungbum Park, and Ju Yong Chang. Representation learning of vertex heatmaps for 3d human mesh reconstruction from multi-view images, 2023. 3
- [3] Hai Ci, Xiaoxuan Ma, Chunyu Wang, and Yizhou Wang. Locally connected network for monocular 3d human pose estimation. *IEEE Transactions on Pattern Analysis and Machine Intelligence*, 44(3):1429–1442, 2020. 4
- [4] Hao-Shu Fang, Jiefeng Li, Hongyang Tang, Chao Xu, Haoyi Zhu, Yuliang Xiu, Yong-Lu Li, and Cewu Lu. Alpha-pose: Whole-body regional multi-person pose estimation and tracking in real-time. *IEEE Transactions on Pattern Analysis and Machine Intelligence*, 2022. 5
- [5] Mohsen Gholami, Ahmad Rezaei, Helge Rhodin, Rabab Ward, and Z Jane Wang. Tripose: A weakly-supervised 3d human pose estimation via triangulation from video. *arXiv preprint arXiv:2105.06599*, 2021. 3
- [6] J. C. Gower. Generalized procrustes analysis. *Psychometrika*, 40(1):33–51, 1975. 3
- [7] Christian Keilstrup Ingwersen, Janus Nørtoft Jensen, Morten Rieger Hannemose, and Anders B. Dahl. Evaluating current state of monocular 3d pose models for golf. In *Proceedings of the Northern Lights Deep Learning Workshop*, 2023. 2, 3, 5
- [8] Christian Keilstrup Ingwersen, Christian Mikkelsen, Janus Nørtoft Jensen, Morten Rieger Hannemose, and Anders Bjørholm Dahl. Sportspose: A dynamic 3d sports pose dataset. In *Proceedings of the IEEE/CVF International Workshop on Computer Vision in Sports*, 2023. 2, 3, 4, 5, 6, 7, 8
- [9] Catalin Ionescu, Dragos Papava, Vlad Olaru, and Cristian Sminchisescu. Human3.6m: Large scale datasets and predictive methods for 3d human sensing in natural environments. *IEEE Transactions on Pattern Analysis and Machine Intelligence*, 36(7):1325–1339, 2014. 3, 4
- [10] Umar Iqbal, Pavlo Molchanov, and Jan Kautz. Weakly-supervised 3d human pose learning via multi-view images in the wild. In *Proceedings of the IEEE/CVF conference on computer vision and pattern recognition*, pages 5243–5252, 2020. 3
- [11] Karim Isakov, Egor Burkov, Victor Lempitsky, and Yury Malkov. Learnable triangulation of human pose. In *International Conference on Computer Vision (ICCV)*, 2019. 3
- [12] Tao Jiang, Peng Lu, Li Zhang, Ningsheng Ma, Rui Han, Chengqi Lyu, Yining Li, and Kai Chen. RTMPose: Real-Time Multi-Person Pose Estimation based on MMPose. *arXiv e-prints*, art. arXiv:2303.07399, 2023. 2
- [13] Hanbyul Joo, Hao Liu, Lei Tan, Lin Gui, Bart Nabbe, Iain Matthews, Takeo Kanade, Shohei Nobuhara, and Yaser Sheikh. Panoptic studio: A massively multiview system for social motion capture. In *2015 IEEE International Conference on Computer Vision (ICCV)*. IEEE, 2015. 2, 3
- [14] Angjoo Kanazawa, Michael J. Black, David W. Jacobs, and Jitendra Malik. End-to-end recovery of human shape and pose. In *2018 IEEE/CVF Conference on Computer Vision and Pattern Recognition*, pages 7122–7131, 2018. 1, 2
- [15] Diederik P Kingma and Jimmy Ba. Adam: A method for stochastic optimization. *arXiv preprint arXiv:1412.6980*, 2014. 4
- [16] Muhammed Kocabas, Salih Karagoz, and Emre Akbas. Self-supervised learning of 3d human pose using multi-view geometry. In *Proceedings of the IEEE/CVF conference on computer vision and pattern recognition*, pages 1077–1086, 2019. 3
- [17] Nikos Kolotouros, Georgios Pavlakos, Michael Black, and Kostas Daniilidis. Learning to reconstruct 3d human pose and shape via model-fitting in the loop. In *2019 IEEE/CVF International Conference on Computer Vision (ICCV)*, pages 2252–2261, 2019. 2
- [18] Kevin Lin, Lijuan Wang, and Zicheng Liu. End-to-end human pose and mesh reconstruction with transformers. In *2021 IEEE/CVF Conference on Computer Vision and Pattern Recognition (CVPR)*, pages 1954–1963, 2021. 2
- [19] Tsung-Yi Lin, Michael Maire, Serge J. Belongie, Lubomir D. Bourdev, Ross B. Girshick, James Hays, Pietro Perona, Deva Ramanan, Piotr Dollár, and C. Lawrence Zitnick. Microsoft COCO: common objects in context. *CoRR*, abs/1405.0312, 2014. 4
- [20] Yanchao Liu, Xina Cheng, and Takeshi Ikenaga. Motion-aware and data-independent model based multi-view 3d pose refinement for volleyball spike analysis. *Multimedia Tools and Applications*, pages 1–24, 2023. 3
- [21] Matthew Loper, Naureen Mahmood, Javier Romero, Gerard Pons-Moll, and Michael J. Black. SMPL: A skinned multi-person linear model. *ACM Trans. Graphics (Proc. SIGGRAPH Asia)*, 34(6):248:1–248:16, 2015. 2, 8
- [22] Dushyant Mehta, Helge Rhodin, Dan Casas, Pascal Fua, Oleksandr Sotnychenko, Weipeng Xu, and Christian Theobalt. Monocular 3d human pose estimation in the wild using improved cnn supervision. In *2017 International Conference on 3D Vision (3DV)*, pages 506–516, 2017. 2, 3
- [23] Rahul Mitra, Nitesh B Gundavarapu, Abhishek Sharma, and Arjun Jain. Multiview-consistent semi-supervised learning for 3d human pose estimation. In *Proceedings of the IEEE/CVF conference on computer vision and pattern recognition*, pages 6907–6916, 2020. 3
- [24] Aiden Nibali, Joshua Millward, Zhen He, and Stuart Morgan. ASPset: An outdoor sports pose video dataset with 3d keypoint annotations. *Image and Vision Computing*, 111: 104196, 2021. 2, 3
- [25] Dario Pavllo, Christoph Feichtenhofer, David Grangier, and Michael Auli. 3d human pose estimation in video with temporal convolutions and semi-supervised training. In *Conference on Computer Vision and Pattern Recognition (CVPR)*, 2019. 2
- [26] N Dinesh Reddy, Laurent Guigues, Leonid Pishchulin, Jayan Eledath, and Srinivasa G. Narasimhan. Tesseract: End-to-end learnable multi-person articulated 3d pose tracking. In *Proceedings of the IEEE/CVF Conference on Computer Vi-*

- sion and Pattern Recognition (CVPR)*, pages 15190–15200, 2021. [3](#)
- [27] Helge Rhodin, Mathieu Salzmann, and Pascal Fua. Unsupervised geometry-aware representation learning for 3d human pose estimation. In *ECCV*, 2018. [4](#)
- [28] Wenkang Shan, Zhenhua Liu, Xinfeng Zhang, Shanshe Wang, Siwei Ma, and Wen Gao. P-stmo: Pre-trained spatial temporal many-to-one model for 3d human pose estimation. In *Computer Vision–ECCV 2022: 17th European Conference, Tel Aviv, Israel, October 23–27, 2022, Proceedings, Part V*, pages 461–478. Springer, 2022. [2](#)
- [29] Karthik Shetty, Annette Birkhold, Srikrishna Jaganathan, Norbert Strobels, Markus Kowarschik, Andreas Maier, and Bernhard Egger. Pliks: A pseudo-linear inverse kinematic solver for 3d human body estimation. In *Proceedings of the IEEE/CVF Conference on Computer Vision and Pattern Recognition (CVPR)*, pages 574–584, 2023. [3](#)
- [30] Ke Sun, Bin Xiao, Dong Liu, and Jingdong Wang. Deep high-resolution representation learning for human pose estimation. In *Proceedings of the IEEE/CVF conference on computer vision and pattern recognition*, pages 5693–5703, 2019. [5](#)
- [31] Timo von Marcard, Roberto Henschel, Michael Black, Bodo Rosenhahn, and Gerard Pons-Moll. Recovering accurate 3d human pose in the wild using imus and a moving camera. In *European Conference on Computer Vision (ECCV)*, 2018. [3](#)
- [32] Jingdong Wang, Ke Sun, Tianheng Cheng, Borui Jiang, Chaorui Deng, Yang Zhao, Dong Liu, Yadong Mu, Mingkui Tan, Xinggang Wang, Wenyu Liu, and Bin Xiao. Deep high-resolution representation learning for visual recognition. *Ieee Transactions on Pattern Analysis and Machine Intelligence*, 43(10):3349–3364, 2021. [2](#)
- [33] Hongyi Xu, Eduard Gabriel Bazavan, Andrei Zanfir, William T Freeman, Rahul Sukthankar, and Cristian Sminchisescu. Ghum & ghuml: Generative 3d human shape and articulated pose models. In *Proceedings of the IEEE/CVF Conference on Computer Vision and Pattern Recognition*, pages 6184–6193, 2020. [2](#)
- [34] Jinlu Zhang, Zhigang Tu, Jianyu Yang, Yujin Chen, and Jun-song Yuan. Mixste: Seq2seq mixed spatio-temporal encoder for 3d human pose estimation in video. In *Proceedings of the IEEE/CVF Conference on Computer Vision and Pattern Recognition (CVPR)*, pages 13232–13242, 2022. [1](#), [2](#)
- [35] Ce Zheng, Sijie Zhu, Matias Mendieta, Taojiannan Yang, Chen Chen, and Zhengming Ding. 3d human pose estimation with spatial and temporal transformers. In *Proceedings of the IEEE/CVF International Conference on Computer Vision (ICCV)*, pages 11656–11665, 2021. [1](#)
- [36] Wentao Zhu, Xiaoxuan Ma, Zhaoyang Liu, Libin Liu, Wayne Wu, and Yizhou Wang. Motionbert: A unified perspective on learning human motion representations. In *Proceedings of the IEEE/CVF International Conference on Computer Vision*, 2023. [1](#), [2](#), [3](#), [4](#), [5](#), [6](#), [8](#)